



Quantitative parameters of dual-layer spectral detector computed tomography for evaluating Ki-67 and human epidermal growth factor receptor 2 expression in colorectal adenocarcinoma

Jinghua Chen^{1#^}, Liang Tang^{1#}, Ping Xie^{2#}, Tingting Qian³, Jian Huang¹, Kefu Liu⁴

¹Department of Radiology, Taicang Hospital of Traditional Chinese Medicine, Taicang, China; ²Department of Ultrasound, The Affiliated Suzhou Hospital of Nanjing Medical University, Suzhou, China; ³Department of Pathology, Taicang Hospital of Traditional Chinese Medicine, Taicang, China; ⁴Department of Radiology, The Affiliated Suzhou Hospital of Nanjing Medical University, Suzhou, China

Contributions: (I) Conception and design: K Liu; (II) Administrative support: K Liu; (III) Provision of study materials or patients: J Chen, T Qian, J Huang; (IV) Collection and assembly of data: J Chen, L Tang, P Xie; (V) Data analysis and interpretation: J Chen, K Liu; (VI) Manuscript writing: All authors; (VII) Final approval of manuscript: All authors.

[#]These authors contributed equally to this work.

Correspondence to: Kefu Liu, MD, PhD. Department of Radiology, The Affiliated Suzhou Hospital of Nanjing Medical University, 242, Guangji Road, Suzhou 215008, China. Email: Liukefu13218190832@163.com.

Background: Ki-67 and human epidermal growth factor receptor 2 (HER2) are key biomarkers in evaluating the prognosis of colorectal adenocarcinoma (CRAC). The purpose of this study was to investigate the value of quantitative parameters in dual-layer spectral detector computed tomography (SDCT) for evaluating the expression of Ki-67 and HER2 in CRAC.

Methods: In this retrospective, cross-sectional study, 88 eligible patients with pathologically confirmed CRAC were selected from Taicang Hospital of Traditional Chinese Medicine between May 2021 and April 2023. The study participants underwent enhanced SDCT of the whole abdomen within 2 weeks before to surgery, did not receive antitumor therapy, and had complete immunohistochemical (IHC) indexes. Patients with nonadenocarcinoma pathologic types, poor quality of spectral CT images, or no complete immunohistochemistry results were excluded. Spectral parameters including CT values at 40 and 100 keV, effective atomic number, iodine concentration (IC), the slope of the spectral Hounsfield unit (HU) curve (λ_{HU}), and normalized iodine concentration (NIC) in the arterial phase (AP) and venous phase (VP) were analyzed for their value in distinguishing between the high and low expression of Ki-67 and HER2-positive and -negative status in CRAC. The statistical significance of the SDCT parameters between the different groups of Ki-67 expression and those of HER2 status was assessed with the Mann-Whitney test. Spearman correlation analysis was used to analyze the correlation between the SDCT parameters and the extent of Ki-67 expression and HER2 expression status. The receiver operating characteristic (ROC) curve was used, and the area under the curve (AUC) was calculated.

Results: The SDCT parameters of CT values at 40 keV, effective atomic number, IC, and the λ_{HU} in the VP showed significant differences between the Ki-67 high- and low-expression groups in CRAC ($P=0.035$, $P=0.041$, $P=0.036$, and $P=0.044$, respectively), with AUCs of 0.639 [95% confidence interval (CI): 0.512–0.766], 0.634 (95% CI: 0.508–0.761), 0.638 (95% CI: 0.510–0.766), and 0.633 (95% CI: 0.504–0.762), respectively. The expression of CRAC Ki-67 was positively correlated with CT values at 40 keV ($r=0.227$; $P=0.034$), effective atomic number ($r=0.219$; $P=0.040$), IC ($r=0.225$; $P=0.035$), and the λ_{HU} in VP ($r=0.216$;

[^] ORCID: 0000-0001-5409-8048.

$P=0.043$). SDCT parameter values showed no statistical difference between negative and positive expression in HER2 (all P values >0.05). There was no significant correlation between SDCT parameters and the expression of HER2 in CRAC (all P values >0.05).

Conclusions: The quantitative parameters of SDCT in the VP provide valuable information for distinguishing between the low expression and high expression of Ki-67 in CRAC.

Keywords: Dual-layer spectral detector CT (SDCT); colorectal adenocarcinoma (CRAC); Ki-67 labeling index; human epidermal growth factor receptor 2 (HER2); quantitative parameters

Submitted Jul 25, 2023. Accepted for publication Nov 08, 2023. Published online Jan 02, 2024.

doi: 10.21037/qims-23-1054

View this article at: <https://dx.doi.org/10.21037/qims-23-1054>

Introduction

Colorectal cancer (CRC) is the third most common cancer in men and the second most common cancer in women, while having the highest cancer mortality in the world (1). The majority of CRC cases are colorectal adenocarcinoma (CRAC) (2).

Nuclear-associated antigen Ki-67, a nuclear proliferation antigen, exists in all cycles of cell mitosis except G0 phase. Ki-67 can be used to evaluate the activity of cell proliferation and is an indicator of tumor malignancy (3). The high expression of Ki-67 is significantly associated with poor overall survival and poor prognosis in patients with CRAC (4). Human epidermal growth factor receptor 2 (HER2) is a transmembrane receptor tyrosine kinase with intrinsic protein tyrosine kinase activity (5). It plays a crucial role in normal cell proliferation, tissue growth, and cancer development by affecting cell migration, proliferation, differentiation, and apoptosis (6). It has been proven to be a potential effective therapeutic target and biomarker for CRAC (7,8).

Dual-layer spectral detector computed tomography (SDCT) can perform multiparameter imaging, quantitative analysis, and energy spectrum analysis of tissues (9), opening up a new field for CT imaging. Through the reconstruction of a spectral-based image dataset obtained via SDCT, virtual monochromatic images (VMIs), iodine concentration (IC), effective atomic number (Z_{eff}) maps, and the slope of spectral Hounsfield unit (HU) curve (λ_{HU}) graph can be obtained (10).

In recent years, studies on SDCT have proliferated (9,10), but there are relatively few reports on SDCT related to CRAC, and only one study (3) has examined the application of SDCT to evaluate the expression of Ki-67 in CRC. Moreover, no research has attempted to evaluate

the diagnostic efficacy of spectral quantitative parameters for predicting the expression status of HER2 in CRAC or to analyze their correlation. If the status of Ki-67 and HER2 can be evaluated before surgery, clinicians can better predict the prognosis of patients with CRAC and formulate the best operation and treatment plan. Therefore, this study aimed to discuss the value of SDCT in predicting the expression status of Ki-67 and HER2 in CRAC. We present this article in accordance with the STROBE reporting checklist (available at <https://qims.amegroups.com/article/view/10.21037/qims-23-1054/rc>).

Methods

Clinical data

A total of 189 cases with pathologically confirmed CRAC were retrospectively analyzed from May 2021 to April 2023 at Taicang Hospital of Traditional Chinese Medicine. The inclusion criteria were as follows: (I) a histological type of CRAC as confirmed by pathology, (II) with complete pathological results and immunohistochemical (IHC) indicators, (III) a satisfactory image quality of SDCT with no obvious artifacts, (IV) no relevant treatment before SDCT examination, (V) no combination with other malignancies, and (VI) an interval between SDCT scanning and pathological immunohistochemistry of less than 2 weeks. The exclusion criteria were as follows: (I) a histopathological type other than adenocarcinoma, (II) no IHC results, (III) an image quality insufficient for evaluation (e.g., severe motion artifacts), (IV) administration of relevant antitumor treatment before enrollment, (V) combination with other malignant tumors, and (VI) an interval between SDCT scan and IHC greater than 2 weeks. The flowchart of the patient selection in this study is shown in *Figure 1*. The

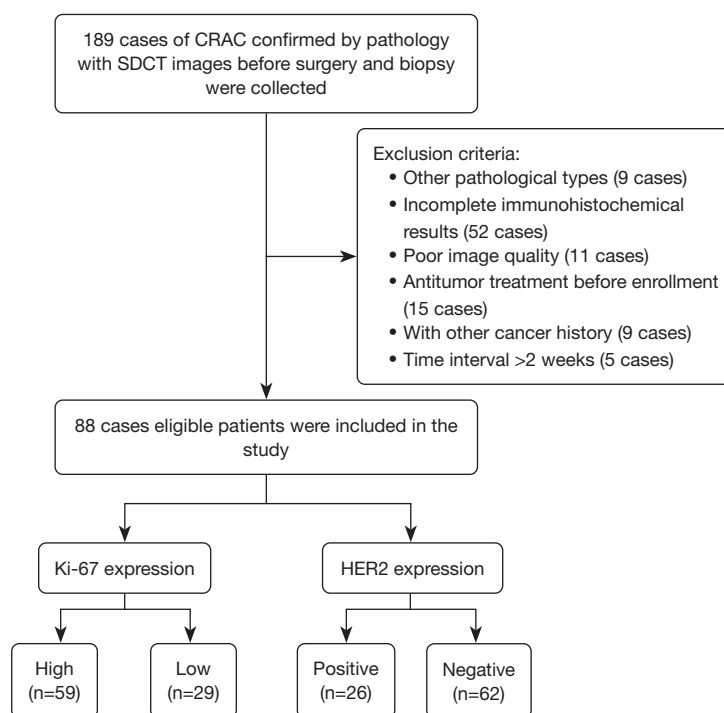


Figure 1 The flowchart of patient selection in this study. CRAC, colorectal adenocarcinoma; SDCT, dual-layer spectral detector CT; CT, computed tomography; HER2, human epidermal growth factor receptor 2.

study was conducted in accordance with the Declaration of Helsinki (as revised in 2013). The ethics committee of Taicang Hospital of Traditional Chinese Medicine approved this study (No. 2021-014), and individual consent was waived due to the retrospective study design.

Ki-67 index evaluation

Ki-67 proliferation index was determined by two pathologists (with 6 and 18 years of pathological work experience, respectively) at high magnification ($\times 400$), who randomly selected 10 fields of view from each slice and recorded 1,000 cells. The staining percentage of Ki-67 receptor was calculated via the semiquantitative method. The Ki-67 index was equal to the Ki-67-positive percentage of the nucleus. According to the median Ki-67 expression index in this study, patients were divided into a Ki-67 high-expression group ($\geq 80\%$ positive cells) and a Ki-67 low-expression group ($< 80\%$ positive cells).

HER2 evaluation

Two pathologists used a four-step scoring method (0, 1+,

2+, 3+) to score immune staining. The IHC staining score scheme was as follows: 0, no staining or $\leq 10\%$ of tumor cells presenting incomplete and weak membrane staining; 1+, $> 10\%$ of tumor cells presenting incomplete and weak membrane staining; 2+, $> 10\%$ tumor cells presenting incomplete and/or weak-to-medium intensity membrane staining (first type) or $\leq 10\%$ of tumor cells presenting strong and complete membrane staining (second type); and 3+, $> 10\%$ of tumor cells presenting strong and complete cell membrane staining. HER2 scores of 2+ and 3+ were considered to be HER2 positive, while scores of 0 and 1+ were considered to be HER2 negative (2,11).

SDCT examination protocol

Scans were performed with an SDCT scanner (IQon spectral CT, Philips Healthcare, Amsterdam, The Netherlands). Patients fasted for 4 to 6 hours before undergoing scanning, and the scanning range was from the top of the diaphragm to the lower edge of the ischial tubercle. The scanning parameters were as follows: tube voltage, 120 kV; automatic tube current control modulation technology (151–193 mA); slice thickness, 5 mm; slice

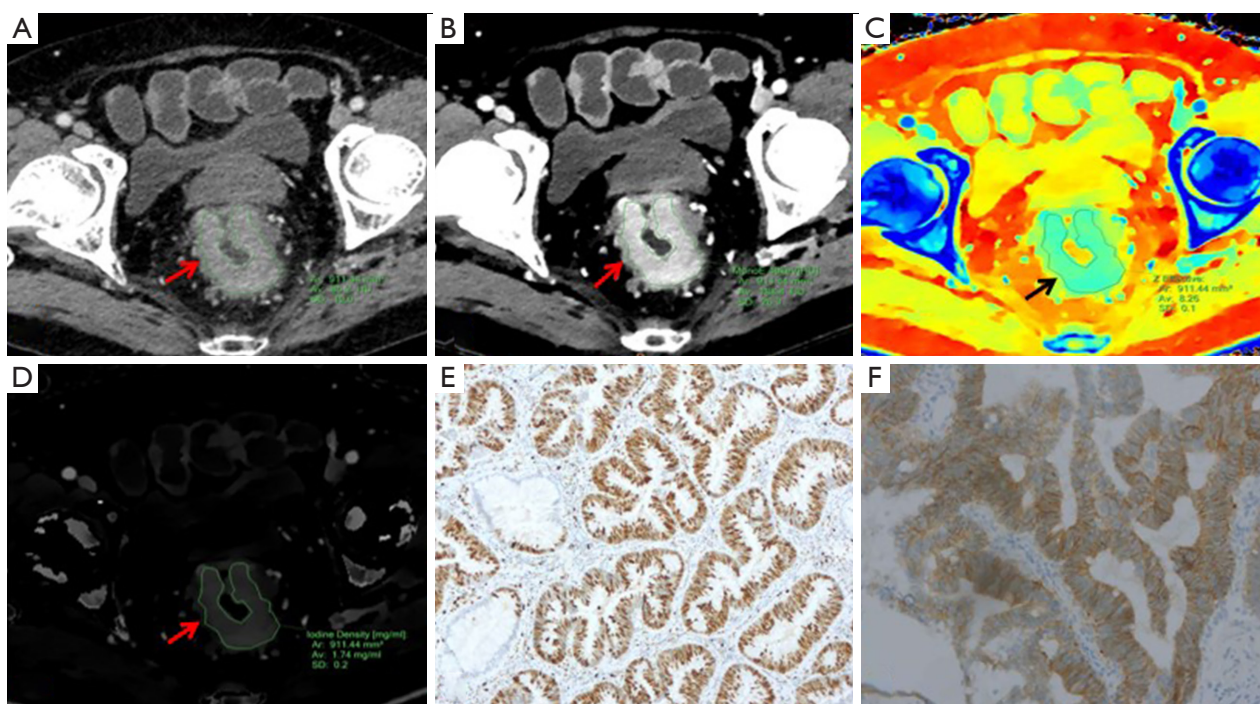


Figure 2 An 81-year-old female with CRAC. (A) The CT value of the lesion was 85.2 ± 19.0 HU in the RT-VP map (red arrow). (B) The CT value of the lesion was 188.4 ± 26.9 HU in the 40-keV-VP map (red arrow). (C) The Zeff value of lesion was 8.26 ± 0.1 in the Zeff-VP map (black arrow). (D) The IC-VP value was 1.74 ± 0.2 mg/mL in the IC-VP map (red arrow). (E) A Ki-67 labeling index of 0.90 (HE, $\times 100$). (F) An HER2 IHC staining score of 3+ (HE, $\times 100$). CRAC, colorectal adenocarcinoma; CT, computed tomography; HU, Hounsfield unit; RT, routine CT; VP, venous phase; Zeff, effective atomic number; IC, iodine concentration; HE, hematoxylin and eosin staining; HER2, human epidermal growth factor receptor 2; IHC, immunohistochemical.

spacing, 5 mm; pitch, 1; field of view, 350 mm; and matrix, 512×512 . The contrast agent ioversol (350 mg/mL; Jiangsu Hengrui Pharmaceuticals Co., Ltd., Lianyungang, China) was injected intravenously through the elbow with a double-tube high-pressure syringe at a dose of 0.8–1.0 mL/kg and an injection rate of 2.5–3.0 mL/s. After injection of contrast agent, 20 mL of normal saline was injected at a flow rate of 3.5 mL/s. Scanning was initiated using the contrast agent autotracking trigger technique. The trigger point of the scan was located in the abdominal aortic cavity. The trigger threshold of the arterial phase (AP) was 150 HU, and the venous phase (VP) was scanned 35 seconds after AP.

Image analysis and data acquisition

The 40-keV VMI, 100-keV VMI, Zeff map, and IC map were reconstructed with a spectral reconstruction algorithm (Spectral Recon Level 4, Philips Healthcare) at an image workstation (IntelliSpace Portal 6.5, Philips Healthcare).

Two radiologists (with 7 and 20 years of experience in abdominal CT images, respectively) performed the independent analysis of SDCT while being blinded to the relevant clinical and pathological information. CRAC tumor margins were first identified in 40-keV VMI images at AP and VP, and then the same level was switched to different spectral images [routine CT (RT), 40-keV VMI, 100-keV VMI, Zeff and IC] to measure the corresponding values, respectively.

λ_{HU} was calculated as the CT attenuation values as follows: $\lambda_{\text{HU}} = (CT_{40\text{keV}} - CT_{100\text{keV}}) / (100 - 40)$.

The normalized iodine concentration (NIC) was calculated as the IC of CRAC (IC_{CRAC}) and the abdominal aorta or external iliac artery (IC_{artery}) at the same slice as CRAC according to the following formula: $\text{NIC} = IC_{\text{CRAC}} / IC_{\text{artery}}$.

The tumor edge was identified in 40-keV VMI images. The region of interest (ROI) was manually outlined at the edge of tumor, with fat, necrosis, blood vessels, and calcification being avoided. The average value on three

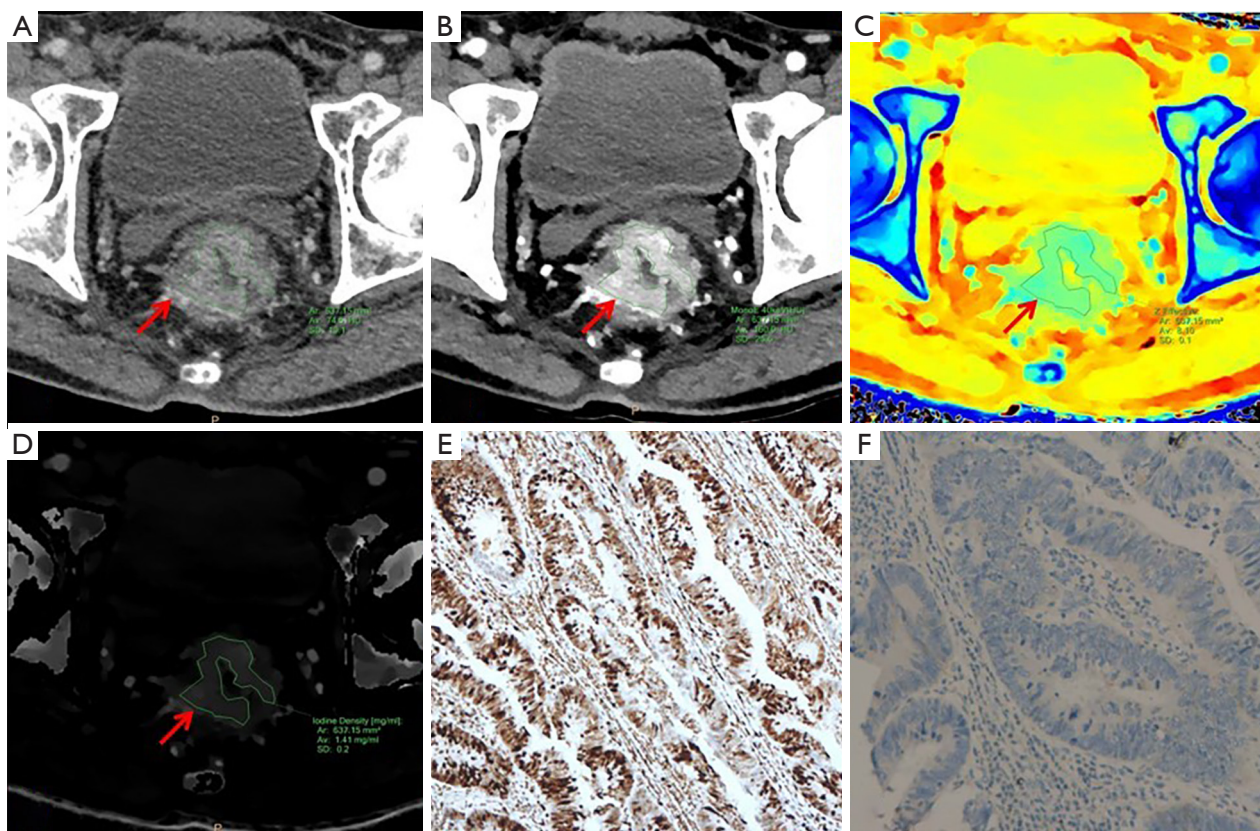


Figure 3 A 55-year-old male with CRAC. (A) The CT value of the lesion was 74.5 ± 19.1 HU in the RT-VP map (red arrow). (B) The CT value of the lesion was 160.0 ± 25.6 HU in the 40-keV-VP map (red arrow). (C) The Zeff value of the lesion was 8.10 ± 0.1 in the Zeff-VP map (red arrow). (D) The IC-VP value was 1.41 ± 0.2 mg/mL in the IC-VP map (red arrow). (E) A Ki-67 labeling index of 0.70 (HE, $\times 100$). (F) An HER2 IHC staining score of 0 (HE, $\times 100$). CRAC, colorectal adenocarcinoma; CT, computed tomography; HU, Hounsfield unit; RT, routine CT; VP, venous phase; Zeff, effective atomic number; IC, iodine concentration; HE, hematoxylin and eosin staining; HER2, human epidermal growth factor receptor 2; IHC, immunohistochemical.

consecutive slices was measured to minimize measurement bias. The ROI was then copied to the same slice of other different spectral parameter maps in the AP and VP images (Figures 2-4).

Statistical analysis

Statistical analysis was calculated with SPSS version 26.0 (IBM Corp., Armonk, NY, USA). Continuous variables are expressed as the mean \pm standard deviation ($\bar{x} \pm SD$). First, the intraclass correlation coefficient (ICC) was used to evaluate the reliability of spectral parameter measurement, and an ICC > 0.75 was considered to have good consistency (12). Statistical significance of the SDCT parameters between the different groups of Ki-67 expression and between the different HER2 status groups was assessed with the Mann-

Whitney test. Spearman correlation analysis was used to analyze the correlation of the SDCT parameters with Ki-67 expression and HER2 expression status. In addition, the receiver operating characteristic (ROC) curve was used, and the area under the curve (AUC) was calculated. The optimal cutoff value was determined according to the Youden index. All examinations were bilateral, and a P value < 0.05 was considered statistically significant.

Results

Clinical characteristics

A total of 88 eligible cases were included in this study, with the clinical characteristics of the included participants being shown in Table 1.

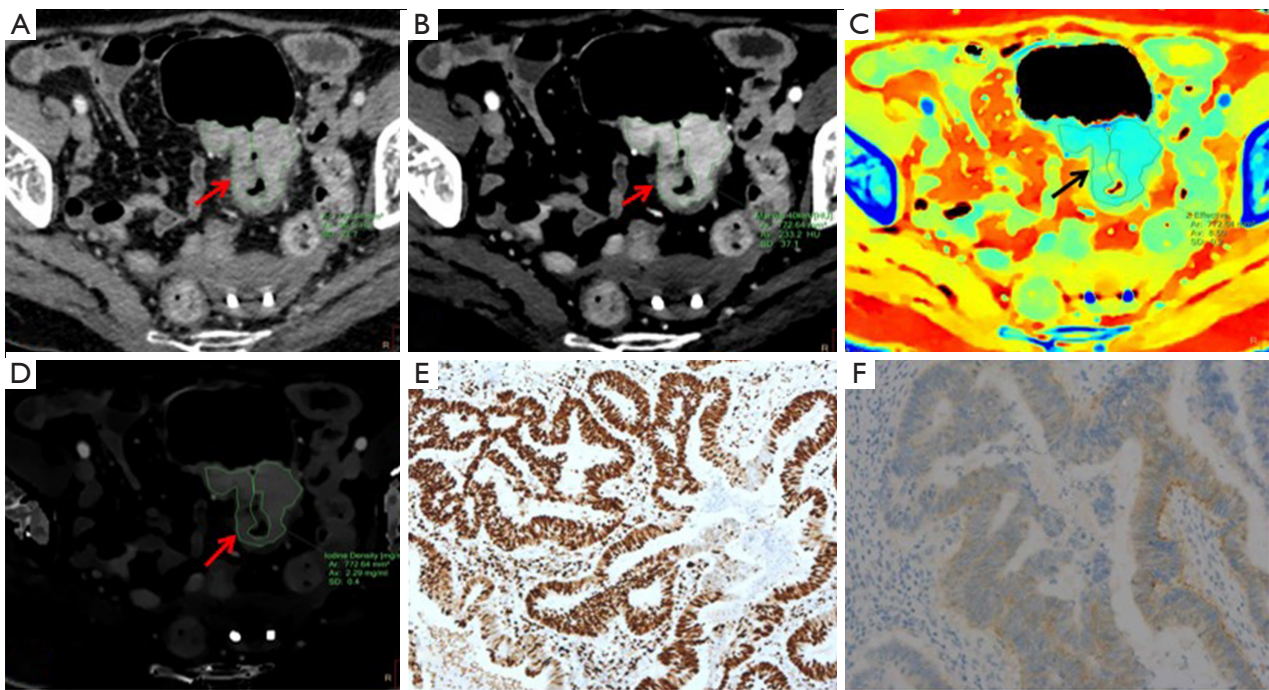


Figure 4 A 76-year-old female with adenocarcinoma of the sigmoid colon. (A) The CT value of the lesion was 96.5 ± 21.7 HU in the RT-VP map (red arrow). (B) The CT value of the lesion was 233.2 ± 37.1 HU in the 40-keV-VP map (red arrow). (C) The Zeff value of the lesion was 8.50 ± 0.2 in the Zeff-VP map (black arrow). (D) The IC-VP value was 2.29 ± 0.4 mg/mL in the IC-VP map (red arrow). (E) A Ki-67 labeling index of 0.85 (HE, $\times 100$). (F) An HER2 IHC staining score of 1+ (HE, $\times 100$). CT, computed tomography; HU, Hounsfield unit; RT, routine CT; VP, venous phase; Zeff, effective atomic number; IC, iodine concentration; HE, hematoxylin and eosin staining; HER2, human epidermal growth factor receptor 2; IHC, immunohistochemical.

Table 1 Clinical characteristics of the included participants

Characteristics	Ki-67		HER2	
	High expression	Low expression	Positive	Negative
Cases, n [%]	59 [67]	29 [33]	26 [30]	62 [70]
Age (years), mean \pm SD	69 ± 10	69 ± 10	70 ± 10	69 ± 10
Male, n	33	15	12	36
Female, n	26	14	14	26
Rectum, n	23	16	12	27
Localization, n				
Ascending/hepatic region	9	2	3	10
Transverse colon	6	3	3	4
Descending/splenic flexure	7	0	1	6
Sigmoid/rectum sigmoid junction	14	8	7	15

HER2, human epidermal growth factor receptor 2; SD, standard deviation.

Table 2 Evaluation on the consistency of spectral parameters measured by two observers

CT parameter	ICC	P value
RT-AP (HU)	0.910	<0.001
40-keV-AP (HU)	0.964	<0.001
100-keV-AP (HU)	0.793	<0.001
Zeff-AP	0.964	<0.001
IC-AP (mg/mL)	0.969	<0.001
NIC-AP	0.978	<0.001
λ_{HU} -AP	0.962	<0.001
RT-VP (HU)	0.964	<0.001
40-keV-VP (HU)	0.972	<0.001
100-keV-VP (HU)	0.861	<0.001
Zeff-VP	0.882	<0.001
IC-VP (mg/mL)	0.958	<0.001
NIC-VP	0.917	<0.001
λ_{HU} -VP	0.968	<0.001

CT, computed tomography; ICC, intraclass correlation coefficient; RT, routine CT; AP, arterial phase; Zeff, effective atomic number; IC, iodine concentration; NIC, normalized iodine concentration; λ_{HU} , slope of the spectral Hounsfield unit curve; VP, venous phase.

Interobserver consistency of the quantitative parameters

Measured values of CRAC spectral quantitative parameters demonstrated good interobserver consistency (ICC range, 0.793–0.978) (Table 2).

The value of SDCT parameters in evaluating the expression of Ki-67

The RT in VP, SDCT parameters of $\text{CT}_{40\text{keV}}$ in VP, Zeff in VP, IC in VP, and λ_{HU} in VP showed significant differences between the Ki-67 high- and low-expression groups in CRAC ($P=0.030$, $P=0.035$, $P=0.041$, $P=0.036$, and $P=0.044$, respectively) (Table 3). Diagnostic efficacy of spectral parameters in distinguishing between the high and low expression of Ki-67 in CRAC were shown in Table 4. The AUCs were 0.639, 0.634, 0.638, and 0.633, respectively. When the cutoffs were 130.3 HU, 8.205, 1.035, and 1.315

Table 3 Comparison of SDCT parameters between the Ki-67 low- and high-expression groups in CRAC (mean \pm SD)

Parameter	Ki-67		Z	P value
	High (n=59)	Low (n=29)		
RT-AP (HU)	61.5 \pm 16.2	61.7 \pm 13.5	-0.022	0.982
40-keV-AP (HU)	104.3 \pm 48.1	109.4 \pm 41.0	-0.386	0.699
100-keV-AP (HU)	49.0 \pm 9.9	49.4 \pm 7.5	-0.067	0.947
Zeff-AP	7.7 \pm 0.3	7.8 \pm 0.3	-0.293	0.770
IC-AP (mg/mL)	0.7 \pm 0.5	0.8 \pm 0.5	-0.297	0.766
NIC-AP	0.1 \pm 0.1	0.1 \pm 0.1	-0.709	0.478
λ_{HU} -AP	0.9 \pm 0.6	1.0 \pm 0.6	-0.315	0.753
RT-VP (HU)	77.9 \pm 15.0	74.5 \pm 12.1	-2.171	0.030*
40-keV-VP (HU)	161.7 \pm 39.9	154.0 \pm 43.6	-2.113	0.035*
100-keV-VP (HU)	57.4 \pm 9.8	55.7 \pm 8.4	-1.798	0.072
Zeff-VP	8.1 \pm 0.3	8.1 \pm 0.3	-2.043	0.041*
IC-VP (mg/mL)	1.4 \pm 0.5	1.3 \pm 0.5	-2.100	0.036*
NIC-VP	0.4 \pm 0.2	0.4 \pm 0.1	-0.373	0.709
λ_{HU} -VP	1.7 \pm 0.6	1.6 \pm 0.7	-2.015	0.044*

*, $P<0.05$. SDCT, dual-layer spectral detector CT; CT, computed tomography; CRAC, colorectal adenocarcinoma; SD, standard deviation; RT, routine CT; AP, arterial phase; Zeff, effective atomic number; IC, iodine concentration; NIC, normalized iodine concentration; λ_{HU} , slope of the spectral Hounsfield unit curve; VP, venous phase.

for $\text{CT}_{40\text{keV}}$ in VP, Zeff in VP, IC in VP, and λ_{HU} in VP, the sensitivities were 94.9%, 39.0%, 94.9%, and 93.2%, respectively, while the specificities were 31.0%, 89.7%, 31.0%, and 34.5%, respectively (Table 4). The expression of Ki-67 in CRAC was positively correlated with RT in VP ($r=0.233$; $P=0.029$), $\text{CT}_{40\text{keV}}$ in VP ($r=0.227$; $P=0.034$), Zeff in VP ($r=0.219$; $P=0.040$), IC in VP ($r=0.225$; $P=0.035$), and λ_{HU} in VP ($r=0.216$; $P=0.043$) (Table 5).

The value of SDCT parameters in evaluating the expression of HER2

SDCT parameter values showed no statistical difference between negative and positive expression in HER2 (all P values >0.05) (Table 6). There was no significant correlation between SDCT parameters and the expression in HER2 in CRAC (all P values >0.05) (Table 7).

Table 4 Diagnostic efficacy of spectral parameters in distinguishing between the high and low expression of Ki-67 in CRAC

Parameters	Youden index	Cutoff, HU	Sensitivity (%)	Specificity (%)	AUC	95% CI	P value
40-keV-VP (HU)	0.259	130.3	94.9	31.0	0.639	0.512–0.766	0.035*
Zeff-VP	0.287	8.205	39.0	89.7	0.634	0.508–0.761	0.041*
IC-VP (mg/mL)	0.259	1.035	94.9	31.0	0.638	0.510–0.766	0.036*
λ_{HU} -VP	0.277	1.315	93.2	34.5	0.633	0.504–0.762	0.044*

*, $P < 0.05$. CRAC, colorectal adenocarcinoma; AUC, area under the curve; CI, confidence interval; VP, venous phase; Zeff, effective atomic number; IC, iodine concentration; λ_{HU} , slope of the spectral Hounsfield unit curve; HU, Hounsfield unit.

Table 5 Correlation between SDCT parameters and the expression of Ki-67 in CRAC

Parameter	Correlation coefficient (r)	P value
RT-AP (HU)	-0.002	0.982
40-keV-AP (HU)	-0.041	0.702
100-keV-AP (HU)	-0.007	0.947
Zeff-AP	-0.031	0.771
IC-AP (mg/mL)	-0.032	0.768
NIC-AP	-0.076	0.482
λ_{HU} -AP	-0.034	0.755
RT-VP (HU)	0.233	0.029*
40-keV-VP (HU)	0.227	0.034*
100-keV-VP (HU)	0.193	0.072
Zeff-VP	0.219	0.040*
IC-VP (mg/mL)	0.225	0.035*
NIC-VP	0.040	0.711
λ_{HU} -VP	0.216	0.043*

*, $P < 0.05$. SDCT, dual-layer spectral detector CT; CT, computed tomography; CRAC, colorectal adenocarcinoma; RT, routine CT; AP, arterial phase; Zeff, effective atomic number; IC, iodine concentration; NIC, normalized iodine concentration; λ_{HU} , slope of the spectral Hounsfield unit curve; VP, venous phase.

Discussion

Studies have found that the 5-year survival rate of CRAC is about 64% (13); however, the 5-year survival rate of metastatic CRAC is only 12% (13,14). Therefore, it is urgent to identify reliable prognostic factors for CRAC. At present, some biomarkers, such as Ki-67 and HER2, have shown promising value in the treatment and prognosis of patients with CRAC. Ki-67 and HER2 are routinely detected via IHC, which requires invasive biopsy or surgery

Table 6 Comparison of SDCT parameters between the positive and negative expression in HER2 in CRAC (mean \pm SD)

Parameter	HER2		Z	P value
	Positive (n=26)	Negative (n=62)		
RT-AP (HU)	66.6 \pm 15.1	59.0 \pm 15.0	-1.907	0.057
40-keV-AP (HU)	118.2 \pm 47.1	103.4 \pm 34.8	-1.244	0.214
100-keV-AP (HU)	50.7 \pm 6.1	48.5 \pm 9.1	-1.866	0.062
Zeff-AP	7.8 \pm 0.3	7.7 \pm 0.3	-1.130	0.259
IC-AP (mg/mL)	0.9 \pm 0.6	0.7 \pm 0.4	-1.171	0.242
NIC-AP	0.1 \pm 0.0	0.1 \pm 0.0	-0.466	0.641
λ_{HU} -AP	1.1 \pm 1.0	0.9 \pm 1.0	-1.024	0.306
RT-VP (HU)	80.2 \pm 18.2	76.5 \pm 15.0	-1.344	0.179
40-keV-VP (HU)	166.2 \pm 58.9	158.7 \pm 39.4	-1.056	0.291
100-keV-VP (HU)	57.5 \pm 10.6	60.0 \pm 7.6	-1.116	0.264
Zeff-VP	8.1 \pm 0.3	8.1 \pm 0.2	-1.185	0.236
IC-VP (mg/mL)	1.5 \pm 0.6	1.4 \pm 0.4	-1.454	0.146
NIC-VP	0.3 \pm 0.0	0.4 \pm 0.0	-1.180	0.238
λ_{HU} -VP	1.7 \pm 1.0	1.8 \pm 1.0	-1.148	0.251

SDCT, dual-layer spectral detector CT; CT, computed tomography; HER2, human epidermal growth factor receptor 2; CRAC, colorectal adenocarcinoma; SD, standard deviation; RT, routine CT; AP, arterial phase; Zeff, effective atomic number; IC, iodine concentration; NIC, normalized iodine concentration; λ_{HU} , slope of the spectral Hounsfield unit curve; VP, venous phase.

to obtain the detection results. Moreover, the biopsy lesions typically are relatively limited, it is easy to miss invasive lesions, and the puncture process can cause tumor metastasis (14). Therefore, an accurate and noninvasive method is needed to predict the expression of Ki-67 and HER2 in patients with CRAC.

Table 7 Correlation between SDCT parameters and the expression of HER2 in CRAC

Parameter	Correlation coefficient (r)	P value
RT-AP (HU)	0.204	0.056
40-keV-AP (HU)	0.133	0.215
100-keV-AP (HU)	0.200	0.062
Zeff-AP	0.121	0.261
IC-AP (mg/mL)	0.126	0.244
NIC-AP	0.050	0.644
λ_{HU} -AP	0.110	0.308
RT-VP (HU)	0.144	0.180
40-keV-VP (HU)	0.113	0.293
100-keV-VP (HU)	0.120	0.267
Zeff-VP	0.127	0.238
IC-VP (mg/mL)	0.156	0.147
NIC-VP	-0.126	0.240
λ_{HU} -VP	0.123	0.253

SDCT, dual-layer spectral detector CT; CT, computed tomography; HER2, human epidermal growth factor receptor 2; CRAC, colorectal adenocarcinoma; RT, routine CT; AP, arterial phase; Zeff, effective atomic number; IC, iodine concentration; NIC, normalized iodine concentration; λ_{HU} , slope of the spectral Hounsfield unit curve; VP, venous phase.

In recent years, SDCT has opened up a new field for CT imaging. Compared with other types of dual-energy CT, SDCT applies noise suppression and iterative algorithm to reduce image noise and improve image quality and can directly generate all spectral datasets without presetting the dual-energy protocol, thus making the clinical workflow more efficient (15,16).

In our study, $\text{CT}_{40\text{keV}}$, Zeff, IC, and λ_{HU} showed significant differences between the Ki-67 high- and low-expression groups in CRAC with $\text{CT}_{40\text{keV}}$ showing the largest AUC for differentiating between the high and low expression of Ki-67 in CRAC. Our result also showed that $\text{CT}_{40\text{keV}}$ in VP, Zeff in VP, IC in VP, and λ_{HU} in VP were positively correlated with the expression of CRAC Ki-67. It has been speculated that this correlation can be attributed to the high expression of Ki-67 being related to the increase in tumor blood supply, which leads to a higher CT value on 40-keV VMI (1,17). Compared with other VMIs, 40-keV VMI exhibits the best signal-to-noise ratio and contrast-to-noise ratio (18,19), which can significantly improve the

detection of lesions, as 40-keV is infinitely close to the 33-keV level of the iodine k edge (20,21).

IC (22) can reflect the vascular conditions and vascular distribution of the tumor. High expression of Ki-67 represents an increase in tumor blood supply, thereby causing an increase in the IC of CRAC (3).

Zeff represents the average atomic number of compounds composed of different components in a tissue, and the evaluation of Zeff can distinguish different tissues that exhibit similar attenuation characteristics at a given energy (23). Tissue with a high Ki-67 high expression indicates more cell proliferation and abnormal angiogenesis than does tissue with a low Ki-67 expression, so the iodine content of the tissue is higher, which results in a higher Zeff value.

Different substances show changes in chemical molecular structure, and different chemical molecules have variable energy attenuation curves (24). This may explain why a high- and low-expression of Ki-67 in CRAC is significantly related to λ_{HU} (17,25).

In our study, $\text{CT}_{40\text{keV}}$, Zeff, IC, and λ_{HU} in VP showed significant differences between the Ki-67 high- and low-expression groups in CRAC, which differs from previous results in which $\text{CT}_{40\text{keV}}$ and IC in AP were significantly different (3). Our findings also indicated that the spectral parameter value in VP could better predict the expression of Ki-67 than that in AP, which was consistent with the results on lung cancer of Dou *et al.* and Zhang *et al.* (26,27). The reason for this may be that the iodine contrast agent in VP can well fill the microvessel and penetrate the basement membrane into the vascular cell space so that the tissue components of CRAC can be optimally contrasted and displayed in VP.

This study did not find that the expression of HER2 was correlated with the spectral parameters of patients with CRAC. We suspect this can be explained by the fact that HER2 protein overexpression only occurs in a small portion of patients with CRAC (2,28). Regardless, the correlation between SDCT parameters and HER2 status needs to be examined by further multicenter and large-sample studies to produce more reliable results.

Some limitations to this study should be mentioned. First, the sample size of this study was small, and a single-center, retrospective design was employed, which could have introduced a degree of selection bias. In the future, we will solve this problem by expanding the sample size and employing a multicenter research design. Second, we only examined CRAC and did not explore other pathological types of CRC. Further research on other pathological types is needed in the future to verify the reliability of the results.

Third, in our study, the number of HER2-positive cases was relatively small, and more cases need to be collected in the future.

Conclusions

SDCT quantitative parameters in VP provides valuable information for distinguishing between the low and high expression of Ki-67 in CRAC. This may help to guide the clinical selection of appropriate treatments.

Acknowledgments

Funding: This study was funded by the Suzhou Key Diseases Project (No. LCZX202212), and the Suzhou Science and Technology Development Plan (Nos. SKY2023064 and SKJYD2021011).

Footnote

Reporting Checklist: The authors have completed the STROBE reporting checklist. Available at <https://qims.amegroups.com/article/view/10.21037/qims-23-1054/rc>

Conflicts of Interest: All authors have completed the ICMJE uniform disclosure form (available at <https://qims.amegroups.com/article/view/10.21037/qims-23-1054/coif>). The authors have no conflicts of interest to declare.

Ethical Statement: The authors are accountable for all aspects of the work in ensuring that questions related to the accuracy or integrity of any part of the work are appropriately investigated and resolved. The study was conducted in accordance with the Declaration of Helsinki (as revised in 2013) and was approved by the Medical Ethics Committee of Taicang Hospital of Traditional Chinese Medicine (No. 2021-014). Individual consent was waived due to the retrospective study design.

Open Access Statement: This is an Open Access article distributed in accordance with the Creative Commons Attribution-NonCommercial-NoDerivs 4.0 International License (CC BY-NC-ND 4.0), which permits the non-commercial replication and distribution of the article with the strict proviso that no changes or edits are made and the original work is properly cited (including links to both the formal publication through the relevant DOI and the license).

See: <https://creativecommons.org/licenses/by-nc-nd/4.0/>.

References

- Li J, Liu ZY, Yu HB, Qu XS, Xue Q, Yu HT, Weeks C. The association between Ki-67 expression and the clinical pathological characteristics of colorectal cancer: A protocol for a systematic review and meta-analysis. *Medicine (Baltimore)* 2020;99:e19996.
- Wang XY, Zheng ZX, Sun Y, Bai YH, Shi YF, Zhou LX, Yao YF, Wu AW, Cao DF. Significance of HER2 protein expression and HER2 gene amplification in colorectal adenocarcinomas. *World J Gastrointest Oncol* 2019;11:335-47.
- Wang YL, Zhang HW, Mo YQ, Zhong H, Liu WM, Lei Y, Lin F. Application of dual-layer spectral detector computed tomography to evaluate the expression of Ki-67 in colorectal cancer. *J Chin Med Assoc* 2022;85:610-6.
- Luo ZW, Zhu MG, Zhang ZQ, Ye FJ, Huang WH, Luo XZ. Increased expression of Ki-67 is a poor prognostic marker for colorectal cancer patients: a meta analysis. *BMC Cancer* 2019;19:123.
- Yan SY, Hu Y, Fan JG, Tao GQ, Lu YM, Cai X, Yu BH, Du YQ. Clinicopathologic significance of HER-2/neu protein expression and gene amplification in gastric carcinoma. *World J Gastroenterol* 2011;17:1501-6.
- Chen J, Li Q, Wang C, Wu J, Zhao G. Prognostic significance of c-erbB-2 and vascular endothelial growth factor in colorectal liver metastases. *Ann Surg Oncol* 2010;17:1555-63.
- Meric-Bernstam F, Hurwitz H, Raghav KPS, McWilliams RR, Fakih M, VanderWalde A, Swanton C, Kurzrock R, Burris H, Sweeney C, Bose R, Spigel DR, Beattie MS, Blotner S, Stone A, Schulze K, Cuchelkar V, Hainsworth J. Pertuzumab plus trastuzumab for HER2-amplified metastatic colorectal cancer (MyPathway): an updated report from a multicentre, open-label, phase 2a, multiple basket study. *Lancet Oncol* 2019;20:518-30.
- Ingold Heppner B, Behrens HM, Balschun K, Haag J, Krüger S, Becker T, Röcken C. HER2/neu testing in primary colorectal carcinoma. *Br J Cancer* 2014;111:1977-84.
- Huang J, Chen J, Wang X, Hao L, Zhang J, Zhang X, Sheng Z, Liu K. The diagnostic value of quantitative parameters on dual-layer detector-based spectral CT in identifying ischaemic stroke. *Front Neurol* 2023;14:1056941.
- Adam SZ, Rabinowich A, Kessner R, Blachar A. Spectral

- CT of the abdomen: Where are we now? *Insights Imaging* 2021;12:138.
11. Valtorta E, Martino C, Sartore-Bianchi A, Penault-Llorca F, Viale G, Risio M, et al. Assessment of a HER2 scoring system for colorectal cancer: results from a validation study. *Mod Pathol* 2015;28:1481-91.
 12. Dillon GA, Lichter ZS, Alexander LM, Vianna LC, Wang J, Fadel PJ, Greaney JL. Reproducibility of the neurocardiovascular responses to common laboratory-based sympathoexcitatory stimuli in young adults. *J Appl Physiol* (1985) 2020;129:1203-13.
 13. Siegel RL, Miller KD, Jemal A. Cancer statistics, 2019. *CA Cancer J Clin* 2019;69:7-34.
 14. Dekker E, Tanis PJ, Vleugels JLA, Kasi PM, Wallace MB. Colorectal cancer. *Lancet* 2019;394:1467-80.
 15. Wen Q, Yue Y, Shang J, Lu X, Gao L, Hou Y. The application of dual-layer spectral detector computed tomography in solitary pulmonary nodule identification. *Quant Imaging Med Surg* 2021;11:521-32.
 16. Hickethier T, Byrtus J, Hauger M, Iuga AI, Pahn G, Maintz D, Haneder S, Doerner J. Utilization of virtual mono-energetic images (MonoE) derived from a dual-layer spectral detector CT (SDCT) for the assessment of abdominal arteries in venous contrast phase scans. *Eur J Radiol* 2018;99:28-33.
 17. Wang P, Tang Z, Xiao Z, Wu L, Hong R, Duan F, Wang Y, Zhan Y. Dual-energy CT in predicting Ki-67 expression in laryngeal squamous cell carcinoma. *Eur J Radiol* 2021;140:109774.
 18. Yuan J, Wang Y, Hu X, Shi S, Zhang N, Wang L, Deng W, Feng ST, Peng Z, Luo Y. Use of dual-layer spectral detector computed tomography in the diagnosis of pancreatic neuroendocrine neoplasms. *Eur J Radiol* 2023;159:110660.
 19. Zeng Y, Geng D, Zhang J. Noise-optimized virtual monoenergetic imaging technology of the third-generation dual-source computed tomography and its clinical applications. *Quant Imaging Med Surg* 2021;11:4627-43.
 20. Nagayama Y, Iyama A, Oda S, Taguchi N, Nakaura T, Utsunomiya D, Kikuchi Y, Yamashita Y. Dual-layer dual-energy computed tomography for the assessment of hypovascular hepatic metastases: impact of closing k-edge on image quality and lesion detectability. *Eur Radiol* 2019;29:2837-47.
 21. Bunch PM, Pavlina AA, Lipford ME, Sachs JR. Dual-Energy Parathyroid 4D-CT: Improved Discrimination of Parathyroid Lesions from Thyroid Tissue Using Noncontrast 40-keV Virtual Monoenergetic Images. *AJNR Am J Neuroradiol* 2021;42:2001-8.
 22. Jiang T, Zhu AX, Sahani DV. Established and novel imaging biomarkers for assessing response to therapy in hepatocellular carcinoma. *J Hepatol* 2013;58:169-77.
 23. Kim C, Kim W, Park SJ, Lee YH, Hwang SH, Yong HS, Oh YW, Kang EY, Lee KY. Application of Dual-Energy Spectral Computed Tomography to Thoracic Oncology Imaging. *Korean J Radiol* 2020;21:838-50.
 24. Xie Y, Zhang S, Liu J, Liang X, Zhang X, Zhang Y, Zhang Z, Zhou J. Value of CT spectral imaging in the differential diagnosis of thymoma and mediastinal lymphoma. *Br J Radiol* 2019;92:20180598.
 25. Cheng SM, Ling W, Zhu J, Xu JR, Wu LM, Gong HX. Dual Energy Spectral CT Imaging in the assessment of Gastric Cancer and cell proliferation: A Preliminary Study. *Sci Rep* 2018;8:17619.
 26. Dou P, Zhao H, Zhong D, Hu Y, Liu B, Zhang H, Cao A. Virtual monoenergetic imaging predicting Ki-67 expression in lung cancer. *Sci Rep* 2023;13:3774.
 27. Zhang Z, Zou H, Yuan A, Jiang F, Zhao B, Liu Y, Chen J, Zuo M, Gong L. A Single Enhanced Dual-Energy CT Scan May Distinguish Lung Squamous Cell Carcinoma From Adenocarcinoma During the Venous phase. *Acad Radiol* 2020;27:624-9.
 28. Li Q, Wang D, Li J, Chen P. Clinicopathological and prognostic significance of HER-2/neu and VEGF expression in colon carcinomas. *BMC Cancer* 2011;11:277.

Cite this article as: Chen J, Tang L, Xie P, Qian T, Huang J, Liu K. Quantitative parameters of dual-layer spectral detector computed tomography for evaluating Ki-67 and human epidermal growth factor receptor 2 expression in colorectal adenocarcinoma. *Quant Imaging Med Surg* 2024;14(1):789-799. doi: 10.21037/qims-23-1054